optica

Magnetic phase diagram of light-mediated spin structuring in cold atoms: supplementary material

G. LABEYRIE[1,*], I. KREŠIĆ[2,3], G. R. M. ROBB[2], G.-L. OPPO[2], R. KAISER[1], AND T. ACKEMANN[2]

[1] Université Côte d'Azur, CNRS, Institut de Physique de Nice, Valbonne, 06560, France
[2] SUPA and Department of Physics, University of Strathclyde,Glasgow G4 0NG, Scotland, UK
[3] Institute of Physics, Bijenička cesta 46, 10000, Zagreb, Croatia
[*] Corresponding author: guillaume.labeyrie@inphyni.cnrs.fr

Published 18 October 2018

This document provides supplementary information to "Magnetic phase diagram of light-mediated spin structuring in cold atoms," https://doi.org/10.1364/OPTICA.5.001322. It includes more information on the theoretical model and numerical results. Section 1 provides the model equations. Section 2 analyzes the pumping of $\Delta m = 2$-coherence. Section 3 provides some numerical evidence for the role played by this coherence in pattern formation.

1. THEORETICAL MODEL

The model is presented in the Supplementary Material of [1] but reproduced here for convenience.

The dynamics of the ground state magnetization is described by optical Bloch equations for the reduced density matrix ρ. A component of the density matrix for states with ground state magnetic quantum numbers $m = i, j$ is denoted by ρ_{ij}. Although the experiment is performed on a $F = 2 \to F' = 3$ transition, the model is developed for a $F = 1 \to F' = 2$ transition, which retains the properties of a $F \to F' = F + 1$ transition as well as both dipole and quadrupole multipole components. We take the quantization axis along the wavevector of the pump beam. Consequently the light fields are expressed in circular components by

$$\mathbf{E}(t) = \frac{1}{2}\sum_{q=\pm1}(-1)^q E_q(t)\hat{\mathbf{e}}_{-\mathbf{q}}e^{i\omega t} + \text{c.c.}, \quad (1)$$

where $\hat{\mathbf{e}}_{\pm}$ are the $\sigma^{\pm}$ polarization unit vectors.

Following the work of [2, 3], we make the following approximations:

- As the decay of the excited state populations and coherences is faster than the ones of the ground state, these are adiabatically eliminated, keeping terms to first order in $\Omega'_{\pm}/\delta$, where $\Omega'_{\pm}$ are the Rabi frequencies of the $\sigma^{\pm}$ fields, and δ is the laser beam detuning.
- Excited state populations are neglected as the pump rate is kept low. Hence the total population remains in the ground state and is constant, giving $\rho_{-1-1} + \rho_{00} + \rho_{11} = 1$.
- Optical coherences are adiabatically eliminated, keeping terms to first order in $\Omega'_{\pm}/\delta$,.
- We use the Landé g-factor $g_F = 0.5$ of the $F = 2$ ground state. The corresponding Larmor frequencies $\Omega_{x,y,z}$ are then given by

$$\Omega_{x,y,z} = \Omega'_{x,y,z}/\Gamma_2 = 0.23 \times B_{x,y,z}/\mathrm{G} \quad (2)$$

  where Γ_2 is the coherence decay rate and half of the atomic linewidth Γ.
- For simplicity in calculating the change in detuning, the Landé factor of the excited state is assumed also to be 0.5.
- In the Raman transition pump rates, detuning changes due to the B_z field are neglected. This approximation is valid as the relevant terms decay with Ω_z on scales much smaller than the detunings used (see Sec. 2 below).

The detuning and the Rabi frequencies are written in units of Γ_2, i.e. $\Delta = \delta/\Gamma_2$ and $\Omega_{\pm} = \Omega'_{\pm}/\Gamma_2$. The pump rates $P_{\pm}$ for the $\sigma_{\pm}$ fields coupling to stretched state transitions $m_1 \to m_{2'}$ and $m_{-1} \to m_{-2'}$ are given by

$$P_{\pm} = \frac{|\Omega_{\pm}|^2}{1 + (\Delta \mp \Omega_z)^2} = \frac{I_{\pm}}{I_{sat}}\frac{2}{1 + (\Delta \mp \Omega_z)^2} \quad (3)$$

where $I_{\pm}$ are the intensities of the circularly polarized components and I_{sat} is the saturation intensity. We consider $\Gamma_2 = \pi \times 6.066$ MHz and $I_{sat} = 1.669$ mW/cm^2 for circular light probing the $F = 2 \to F' = 3$ transition of the D$_2$ line of ^{87}Rb for all atoms in the stretched state $|m| = 2$ (see [4]). We also consider the sum and difference pump rates $\mathcal{S} = P_+ + P_-$, $\mathcal{D} = P_+ - P_-$.

The Raman transition pump rates $P_{\Lambda\pm}$ driving the $|\Delta m| = 2$ coherence are given by

$$P_{\Lambda+} = \frac{2\,\mathrm{Re}(\Omega_+^*\Omega_-)}{1+\Delta^2},\ P_{\Lambda-} = -\frac{2\,\mathrm{Im}(\Omega_+^*\Omega_-)}{1+\Delta^2}. \quad (4)$$

Defining the system variables as

$$\begin{aligned}
u &= \rho_{-11} + \rho_{1-1},\\
v &= i(\rho_{-11} - \rho_{1-1}),\\
w &= \rho_{11} - \rho_{-1-1},\\
X &= \rho_{11} + \rho_{-1-1} - 2\rho_{00},\\
y_1 &= \rho_{-10} + \rho_{0-1},\\
z_1 &= \rho_{01} + \rho_{10},\\
y_2 &= i(\rho_{-10} - \rho_{0-1}),\\
z_2 &= i(\rho_{01} - \rho_{10}),
\end{aligned} \quad (5)$$

we derive a set of 8 coupled evolution equations (where $(\dot{}) \equiv \frac{d}{dt}()$):

$$\begin{aligned}
\dot{u} &= -\Gamma_c u + \left(2\Omega_z + \tfrac{5}{6}\mathcal{D}\Delta\right) v + \tfrac{1}{6}P_{\Lambda-}\Delta w - \tfrac{1}{9}P_{\Lambda+}X + \tfrac{5}{18}P_{\Lambda+}\\
&\quad -\Omega_x(z_2 - y_2)/\sqrt{2} + \Omega_y(z_1 - y_1)/\sqrt{2},\\
\dot{v} &= -\Gamma_c v - \left(2\Omega_z + \tfrac{5}{6}\mathcal{D}\Delta\right) u + \tfrac{1}{6}P_{\Lambda+}\Delta w + \tfrac{1}{9}P_{\Lambda-}X - \tfrac{5}{18}P_{\Lambda-}\\
&\quad +\Omega_x(z_1 - y_1)/\sqrt{2} + \Omega_y(z_2 - y_2)/\sqrt{2},\\
\dot{w} &= -\Gamma_w w - \tfrac{1}{6}P_{\Lambda-}\Delta u - \tfrac{1}{6}P_{\Lambda+}\Delta v - \tfrac{1}{9}\mathcal{D}X + \tfrac{5}{18}\mathcal{D}\\
&\quad -\Omega_x(y_2 + z_2)/\sqrt{2} - \Omega_y(y_1 + z_1)/\sqrt{2},\\
\dot{X} &= -\Gamma_X X - \tfrac{1}{3}P_{\Lambda+}u + \tfrac{1}{3}P_{\Lambda-}v + \tfrac{1}{3}\mathcal{D}w + \tfrac{5}{18}\mathcal{S}\\
&\quad +3\Omega_x(y_2 - z_2)/\sqrt{2} + 3\Omega_y(y_1 - z_1)/\sqrt{2},\\
\dot{y}_1 &= -\Gamma_y y_1 + (\Omega_z + \Delta\mathcal{D}_y)y_2 + \left(\tfrac{P'_-}{6} + \tfrac{1}{12}\left(\Delta P_{\Lambda-} - P_{\Lambda+}\right)\right) z_1\\
&\quad + \left(\tfrac{\Delta P'_-}{6} + \tfrac{1}{12}\left(\Delta P_{\Lambda+} + P_{\Lambda-}\right)\right) z_2\\
&\quad +\Omega_x v/\sqrt{2} + \Omega_y(w - x + u)/\sqrt{2},\\
\dot{y}_2 &= -\Gamma_y y_2 - (\Omega_z + \Delta\mathcal{D}_y)y_1 - \left(\tfrac{\Delta P'_-}{6} - \tfrac{1}{12}\left(\Delta P_{\Lambda+} + P_{\Lambda-}\right)\right) z_1\\
&\quad + \left(\tfrac{P'_-}{6} + \tfrac{1}{12}\left(P_{\Lambda+} - \Delta P_{\Lambda-}\right)\right) z_2\\
&\quad +\Omega_x(w - x - u)/\sqrt{2} + \Omega_y v/\sqrt{2},\\
\dot{z}_1 &= -\Gamma_z z_1 + (\Omega_z + \Delta\mathcal{D}_z)z_2 + \left(\tfrac{P'_+}{6} - \tfrac{1}{12}\left(\Delta P_{\Lambda-} + P_{\Lambda+}\right)\right) y_1\\
&\quad - \left(\tfrac{\Delta P'_+}{6} + \tfrac{1}{12}\left(\Delta P_{\Lambda+} - P_{\Lambda-}\right)\right) y_2\\
&\quad -\Omega_x v/\sqrt{2} + \Omega_y(w + x - u)/\sqrt{2},\\
\dot{z}_2 &= -\Gamma_z z_2 - (\Omega_z + \Delta\mathcal{D}_z)z_1 + \left(\tfrac{\Delta P'_+}{6} - \tfrac{1}{12}\left(\Delta P_{\Lambda+} - P_{\Lambda-}\right)\right) y_1\\
&\quad + \left(\tfrac{P'_+}{6} + \tfrac{1}{12}\left(\Delta P_{\Lambda-} + P_{\Lambda+}\right)\right) y_2\\
&\quad +\Omega_x(w + x + u)/\sqrt{2} - \Omega_y v/\sqrt{2}.
\end{aligned} \quad (6)$$

The decay rates of the atomic variables are

$$\begin{aligned}
\Gamma_w &= r + \frac{1}{6}(P_+ + P_-), && (7)\\
\Gamma_X &= r + \frac{11}{18}(P_+ + P_-), && (8)\\
\Gamma_c &= r + \frac{7}{6}(P_+ + P_-) && (9)\\
&\quad - \frac{|\Omega_+|^2 + |\Omega_-|^2}{3\,(1+\Delta^2)}, && (10)\\
\Gamma_y &= r + P'_+ + \frac{7}{12}P'_- && (11)\\
\Gamma_z &= r + \frac{7}{12}P'_+ + P'_-, \text{ with} && (12)\\
P'_\pm &= \frac{|\Omega_\pm|^2}{1 + (\Delta \mp 2\Omega_z)^2}, && (13)
\end{aligned}$$

where r is an effective decay rate of the Zeeman ground state population and coherences. Its lower limit results from the residual atomic motion leading to a wash-out of the structures and can be estimated to be about $2.8 \times 10^3\mathrm{s}^{-1}$, i.e. $r \approx 1.5 \times 10^{-4}$ in the scaled units used here. The difference pump rates in the light-shift terms for y_1, y_2, z_1, z_2 are

$$\mathcal{D}_y = P'_+ - \tfrac{7}{12}P'_-, \quad \mathcal{D}_z = \tfrac{7}{12}P'_+ - P'_-. \quad (14)$$

We have derived an expression for the non-linear optical response of the atoms in the same framework as above (see Eq. (1) of the main paper). Using this optical response, the equations for the evolution of the amplitudes $E_\pm$ of the forward beam through the diffractively thin cloud are

$$\tfrac{\partial}{\partial z}E_\pm = i\chi_\pm \tfrac{k}{2}\left[\left(1 \pm \tfrac{3}{4}w + \tfrac{1}{20}X\right)E_\pm + \tfrac{3}{20}(u \mp iv)E_\mp\right], \quad (15)$$

where the linear susceptibility $\chi_\pm$ is

$$\chi_\pm = \frac{OD}{kL}\frac{i + \Delta \mp \Omega_z}{1 + (\Delta \mp \Omega_z)^2}, \quad (16)$$

where OD is the optical density, since in simulations we include both light absorption and refraction, and the linear and non-linear Faraday effects. Formulas (15) and (16) are used in the main paper with un-normalized variables.

After traversing the cloud, the beams propagate a distance of two times the mirror distance d (to the feedback mirror and back), which is governed by

$$\frac{\partial}{\partial z}E_\pm = -\frac{i}{2k}\Delta_\perp E_\pm, \quad (17)$$

where $\Delta_\perp$ is the transverse Laplacian. We take the interacting Rabi frequencies as the sum of the forward field at the entrance of the medium and the reentrant field at the exit field of the medium calculated from Eqs. (15), (17) neglecting the wavelength-scale grating resulting from the interference of counterpropagating fields. Both assumptions proved to be suitable in earlier studies in cold atoms [5]. In particular, as the dynamics is evolving on time scales of the order of $1/r$ and the period of the wavelength scale grating is about a factor of 100 smaller than the pattern period, atomic motion is expected to provide a strong damping to the wavelength-scale modulations (Supplementary material of [5]). The details of numerical procedures used in our simulations are given in Ref. [6].

2. ROLE OF $\Delta M = 2$-COHERENCE

The complete solution of the system (6) is out of the scope of this paper, but important insight on the role of the coherences and the associated magnetic quadrupoles can be drawn already from an inspection of the equations of motion for the coherence $\Phi = u + iv$ alone, neglecting the coupling to other moments and the light shift terms:

$$\dot{u} = -\Gamma_c u + 2\Omega_z v + \frac{5}{18} P_{\Lambda+} \quad (18)$$

$$\dot{v} = -\Gamma_c v - 2\Omega_z u - \frac{5}{18} P_{\Lambda-} \quad (19)$$

The stationary solutions of these equations are

$$u = \frac{5}{18} \frac{\Gamma_c}{\Gamma_c^2 + 4\Omega_z^2} \left(P_{\Lambda+} - 2\frac{\Omega_z}{\Gamma_c} P_{\Lambda-} \right) \quad (20)$$

$$v = -\frac{5}{18} \frac{\Gamma_c}{\Gamma_c^2 + 4\Omega_z^2} \left(P_{\Lambda-} + 2\frac{\Omega_z}{\Gamma_c} P_{\Lambda+} \right) \quad (21)$$

The first thing to note is that the longitudinal field is destroying the coherence as the levels become non-degenerate. This happens if the longitudinal field is of the order of Γ_c which in term depends on the total input intensity. This explains, for Ω_z, the statement in the main text that the extent of the phases in magnetic space increases with increasing input power. A corresponding relation can be derived for the transverse field and w.

The second point to note is that the longitudinal field provides a symmetry breaking for v. The dominant terms is $\Omega_z P_{\Lambda+}/\Gamma_c$, which results from the precession of the u generated by the pump into the v direction due to the longitudinal field. The corrections for $P_{\Lambda+}$, $P_{\Lambda-}$ including the linear Faraday effect (Ω_z dependence in Eq. (16)) scale only like Ω_z/Δ. Also the symmetry breaking due to the Zeeman shifts in the denominators of pump rates, Eq. 3), scale like Ω_z/Δ (nonlinear Faraday effect). As discussed in the paragraph before, the coherences are relevant for $|\Omega_z| \lesssim \Gamma_c < 0.1$ (for the parameters of Fig. 2 of the main paper). As $|\Delta| \approx 14$, the symmetry breaking due the linear and nonlinear Faraday effect is small in this regime. (In particular, this also justifies that it is no problem that the Ω_z dependence of the Raman pump rates in Eq. (4) is neglected. It is dominated by the coherent precession dynamics in the region where the coherences are important.) We anticipate that the transition between the AM/FM phases with well developed symmetries and high modulation depth to the high B_z-phase is related to the decay of the coherences. A more detailed theoretical investigation is ongoing. Note that a homogeneous components of v can help to drive the w dynamics via the $P_{\Lambda+}\Delta v$. Hence the phases can be still w-driven but v-enhanced.

Taking the field as a superposition of Ω_+ and $\Omega_- \exp(-\phi_L)$ with Ω_+, Ω_- real and ϕ_L denoting the phase difference, one obtains for the Raman pump rates

$$P_{\Lambda+} = \frac{2\Omega_+\Omega_-}{1+\Delta^2} \cos\phi_L \quad (22)$$

$$P_{\Lambda-} = \frac{2\Omega_+\Omega_-}{1+\Delta^2} \sin\phi_L, \quad (23)$$

and for the stationary solutions

$$u = \frac{5}{18} \frac{\Gamma_c}{\Gamma_c^2 + 4\Omega_z^2} \frac{2\Omega_+\Omega_-}{1+\Delta^2} \left(\cos\phi_L - 2\frac{\Omega_z}{\Gamma_c} \sin\phi_L \right) \quad (24)$$

$$v = -\frac{5}{18} \frac{\Gamma_c}{\Gamma_c^2 + 4\Omega_z^2} \frac{2\Omega_+\Omega_-}{1+\Delta^2} \left(\sin\phi_L + 2\frac{\Omega_z}{\Gamma_c} \cos\phi_L \right) \quad (25)$$

$$\Phi = \frac{5}{18} \frac{\Gamma_c}{\Gamma_c^2 + 4\Omega_z^2} \frac{2\Omega_+\Omega_-}{1+\Delta^2} e^{-i\phi_L} \left(1 - i2\frac{\Omega_z}{\Gamma_c} \right). \quad (26)$$

This shows that the phase ϕ_L between the circular polarization components determines the phase of the coherence Φ. The angle of the polarization direction with respect to the x-axis, ϕ_p, for linearly polarized light (or the principal axis for $\Omega_+ \neq \Omega_-$) is related to half the phase difference as the phase ϕ_L varies between 0 and 2π but the polarization direction ϕ_p only between 0 and π:

$$\phi_p = \frac{\phi_L - \pi}{2}. \quad (27)$$

The direction of the principal axis of the quadrupole ϕ_Q is linked to the phase of the coherence via an equation like (27). Hence the polarization direction of the light is directly controlling the direction of the quadrupole, $\phi_p = \phi_Q$, which is of course expected from symmetry arguments. For example, in the notation used the x-polarized input beam corresponds to $\phi_L = \pi$ and $\phi_p = 0$. It pumps (for $\Omega_z = 0$), $u \neq 0$, $v = 0$, i.e. the lobes of the resulting quadrupole (representation of u in Fig. 1a of the main article) are directed along the x-axis, the orthogonal lobes along y. $\phi_L = \pi/2$ corresponds to light polarized at 45° to the x-axis. It pumps (for $\Omega_z = 0$), $u = 0$, $v \neq 0$, i.e. the lobes of the resulting quadrupole (representation of v in Fig. 1a of the main paper) are directed at ± 45° along the bisections of the x-axis and y-axis. In between, there is a smooth transition stemming from the form of the spherical harmonic function. A situation with $\phi_L = \pi/4$ corresponding to a polarization direction of -22.5° gives $u = v$. Hence also the quadrupole axes will point in the direction intermediate to the two cases plotted in Fig. 1a of the main paper, i.e. will be at -22.5° and 67.5°. We will discuss consequences for the modulated magnetic state below.

3. DETAILS ON NUMERICAL EVIDENCE OF COHERENCE BASED PHASE

For numerical tests, we compare the modulation depth of the v variable for $B_x = 0$ and $B_x = 1$ G. The $v = \mathrm{Im}(\Phi)$ profile inside the cloud is shown in Fig. 1, for the two cases. Fig. 1(a) shows the square structure characteristic of the $B_x = 0$ phase. These structures exist in the spin-1/2 model [7, 8], and the v variable is here not significant, as witnessed in the weak steady state modulation depth of $\Delta v = 0.032$. A markedly different v distribution is shown in the image Fig. 1(b). The disordered structure is characteristic for the high $|B_x|$ phase, as shown in Fig. 3 of the main paper. The modulation depth is now equal to $\Delta v = 0.29$, nearly an order of magnitude larger than the value measured for the square structure.

Fig. 1c) shows a cut through the distribution of v obtained from numerical simulations (in this plot Λ is the typical spatial period of the pattern). From the phase of $u + iv$, the angle of the resulting quadrupole moment in the $x - y$-plane is obtained. Where $v = 0$, $\phi_Q = 0$, i.e. the principal axis of the quadrupole is along the x-axis as only the u component from the homogeneous pumping is present. Positive, respectively negative excitation of v leads to a rotation of the quadrupole in the corresponding direction. Maximum excursion is about 23°, about half way the

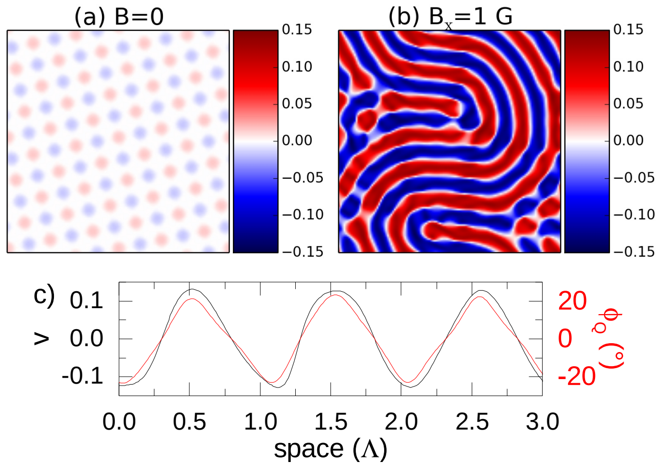

Fig 1. Numerical evidence for a strong v modulation in the high $|B_x|$ phase. Transverse profile of the v variable for (a) $B_x = 0$ and (b) $B_x = 1$ G. Simulation parameters: $OD = 70$, pump intensity $I = 0.4\, I_{sat}$ and detuning $\delta = -8\,\Gamma_2$. c) Illustration of modulated quadrupole pattern obtained from numerical simulations. Black line: Cut through the imaginary part of the coherence v orthogonal to the local stripe pattern in the lower center part of panel (b). Red line: Direction of the principal axis of the quadrupole obtained from the phase of $u + iv$ and applying Eq. (27) for ϕ_Q instead of ϕ_P.

full excursion to 45° (corresponding to the v moment alone), as in the peaks $|v/u| \approx 1$. This corresponds to a magnetic ordered structure in which the direction of the quadrupole is oscillating in space. The deviations between the shape of the v and the ϕ_Q curves are due to the fact that in the structured state also u is modulated.

REFERENCES

1. I. Kresic, G. Labeyrie, G. R. M. Robb, G.-L. Oppo, P. M. Gomes, P. Griffin, R. Kaiser, and T. Ackemann, Commun. Phys. (in press, 2018).
2. F. Mitschke, R. Deserno, W. Lange,and J. Mlynek, Phys. Rev. A **33**, 3219 (1986).
3. J. Dalibard and C. Cohen-Tannoudji, J. Opt. Soc. Am. B **6**, 2023 (1989).
4. D. A. Steck, *Rubidium 87 D Line Data*, available online at http://steck.us/alkalidata (revision 2.1.4, 23 December 2010).
5. G. Labeyrie, E. Tesio, P.M. Gomes, G.-L. Oppo, W.J. Firth, G.R.M. Robb, A.S. Arnold, R. Kaiser and T. Ackemann, Nat. Photonics **8**, 321 (2014).
6. E. Tesio, *Theory of self-organization in cold atoms*, PhD Thesis, University of Strathclyde (2014).
7. A. J. Scroggie and W. J. Firth, Phys. Rev. A **53**, 2752 (1996).
8. A. Aumann, E. Büthe, Yu. A. Logvin, T. Ackemann, and W. Lange, Phys. Rev. A **56**, R1709 (1997).